Pergamon

Int. J. Solids Structures Vol. 32, No. 17/18, pp. 2423–2445, 1995

0020–7683/95 $9.50 + .00

0020–7683(94)00275–4

RESEARCH CHALLENGES ARISING FROM CURRENT AND POTENTIAL APPLICATIONS OF DYNAMIC FRACTURE MECHANICS TO THE INTEGRITY OF ENGINEERING STRUCTURES

M. F. KANNINEN
Structural Systems and Technology Division, Southwest Research Institute, San Antonio, TX, U.S.A.

and

P. E. O'DONOGHUE
Department of Civil Engineering, University College, Dublin, Ireland

(*Received* 3 *February* 1994)

Abstract—Following several decades of contentiousness, the general framework of dynamic fracture mechanics is now generally agreed upon. While some basic issues remain unresolved, many successful practical applications have been made. Examples are provided in this paper that are drawn from the transport of fluids in gas pipelines, and of people in aircraft and aerospace vehicles. These examples illustrate that the changing trend in research and development, in which a much greater emphasis is now being placed on short-range practical applications, can nonetheless identify and stimulate basic research. Research challenges emerging from the dynamic fracture mechanics applications outlined in this paper are provided to support this contention.

1. INTRODUCTION

There are two major trends in the United States that impact the subject of dynamic fracture mechanics. The first is that the nation's energy, communication and transportation infrastructure is aging at a time when the economic climate and societal priorities are impeding replacements and refurbishments. The second trend is that the nature of research and development is undergoing a sea change by moving away from long-term basic research towards a concentration on near-term pragmatic applied research. It is amply apparent that opportunities to partake in small, narrowly focused, basic research projects that only provide results of scholarly value are currently diminishing.

Both governmental and industrial organizations are now most interested in supporting applied research of a kind that will provide pragmatic near-term results, because it is needed to help them support their customers. Products that can be marketed to enhance their revenue, along with practical procedures that can save them money in installation, operation and maintenance of revenue producing equipment, are currently most prized by organizations that support research. Learned research papers published in eminent scientific and engineering journals are not.

Notwithstanding the negative long-term impact that it surely will have on the quality of the technology (and its practitioners) when the new millennium commences, there is little point in resisting the undeniable trend towards applied research. A more productive course is to work within the constraints imposed by the current research and development funding situation, but without completely capitulating to them. By bringing the best level of current technology that is appropriate to resolve technical obstacles within a given application area, it should be possible to identify underlying issues that must be addressed with long-term basic research. Research that eliminates "show stoppers", that can be justified in the context of providing the benefits that government/industry organizations require, may then become attractive enough to receive support also. The primary aim of this paper is to stimulate this process.

A secondary aim of this paper is to alter a myopic view held by some that dynamic fracture mechanics is a narrow esoteric field. Indeed, many highly proficient researchers with their focus exclusively on fundamental mechanisms unwittingly add to this perception. This paper attempts to balance such views by showing that, while there surely are areas where insufficient knowledge exists to quantify dynamic failures in engineering terms, there are also ample successful practical application areas. As a compromise between breadth and depth in the treatment, this paper will select pertinent examples from the aging of the transportation infrastructure, with specific emphasis being given to pipelines.

Gas and oil, which together currently supply some 68% of the world's energy needs (Ensley, 1994), both pass through pipelines in their movement from source to usage. It should not be surprising, therefore, that the U.S.A. now has over 300,000 miles of crude oil pipelines with about 800,000 miles of natural gas gathering, transmission and distribution piping. A significant fraction of these systems has exceeded its nominal design life. Moreover, recent regulatory action that has made pipeline companies become common carriers has acerbated operational demands, e.g. through more frequent pressure cycles than can accelerate stress corrosion cracking. There is obvious concern with regard to the continuity of service, to the cost of replace and repair operations, and the danger to the environment and to the public should a failure occur. More to the point of this paper, because the causes of failure initiation and/or the mechanisms associated with subsequent behavior often involve dynamic events, appropriate application of dynamic fracture mechanics can have a very significant societal benefit.

2. DYNAMIC FRACTURE MECHANICS BACKGROUND

There are three general types of dynamic failure problems: (1) the perforation of an initially homogeneous body from mechanical impact or other source of dynamic loading; (2) the initiation of crack propagation under rapidly applied loading; and (3) the rapid propagation and arrest of a crack under fixed or slowly varying applied loading. This paper will be limited to situations in which a single dominant crack-like defect exists (or can be postulated) in the structure under consideration. Generally encompassing events that occur in the order of milliseconds, these situations include the sudden initiation, rapid propagation and arrest of a dominant crack that may also turn, bifurcate, pause and reinitiate.

While these problems can be addressed using the methodology of dynamic fracture mechanics [see Kanninen and Popelar (1985); Freund (1990); Kanninen and Atluri (1986); Knauss and Rosakis (1990)], an initially homogeneous (or at least coherent heterogenous body in the macroscopic sense) that precipitively separates along a narrow boundary to become a crack cannot now be quantified in continuum fracture mechanics terms. This area, which has progressed only marginally beyond the classic papers of Gurney (1943) and Taylor (1963), is not currently addressed by dynamic fracture mechanics.

Dynamic fracture mechanics processes are of most interest when they cause failure—the inability of a structure to fulfil its intended function. In this paper failure is associated with a crack that penetrates a load bearing element such that the remaining uncracked material is no longer able to carry the required load, and/or one that perforates a boundary such that the fluid being contained by it egresses through the opening at an unacceptable rate. Quantitatively, rapid crack initiation and propagation are governed by an equality between the dynamically computed crack driving force and the resistance of the material to crack extension. For small scale yielding conditions, this is expressible as

$$K(a, \sigma, t) = K_D(V, T, B). \tag{1}$$

In eqn (1), K_D is the experimentally determined dynamic (or running) fracture toughness, a material property that depends on component thickness B, crack speed V and the temperature T. In contrast, K is the dynamically calculated value of the stress intensity factor, a function of crack length a, applied stress σ, time t, as well as the component configuration.

As a special case of eqn (1), crack arrest occurs when K becomes less than the minimum value of K_D, and remains less for some long period of time, i.e. when

$$K(t) < (K_D)_{min} \quad \text{as} \quad t \to \infty. \tag{2}$$

Under small scale yielding conditions the quantity $(K_D)_{min}$ is conventionally referred to as K_a, the crack arrest toughness, and it is equal to K_d, the initiation toughness for the limiting case of a very rapidly applied loading. For dynamically propagating cracks, with the exception of a few very simple cases, dynamic stress intensity factors must be computed using elastodynamic computational procedures. It is also important to recognize that, even in elastodynamic conditions, the appropriate material fracture toughness parameters are not directly accessible through experimental measurements, but must be deduced from measurements with the aid of some type of analysis procedure.

Equation (1) follows from the crack tip dominance argument that is the basis of modern fracture mechanics (Kanninen and Popelar, 1985; Freund, 1990). When small scale yielding is not appropriate, either in the material fracture propagation experiments and/or in the application itself, K will not "dominate" the inelastic region at the crack tip. It is then necessary to include inelastic behavior explicitly. This introduces complexities beyond widespread plastic deformation such as the possibility of strain rate-dependent behavior in the crack tip region. While many generalized parameters have been proposed as inelastic-dynamic fracture criteria, none are completely satisfactory. The more promising of these criteria are based on crack tip integrals; one of these being the inelastic-dynamic G parameter developed by Moran and Shih (1987). However, it has been found that the crack tip integral formulations are encompassed by a general class of integrals, denoted by T^*, that were introduced by Atluri and his co-workers (Atluri, 1982; Brust, 1985). The T^* integral is given by

$$T^* = \sum_{k=1}^{m} \Delta T^* \tag{3a}$$

which in expanded form can be written as

$$T^* = \sum_{k=1}^{m} \left\{ \lim_{\Gamma \to 0} \int_{\Gamma} [(\Delta W + \Delta P) n_1 - (\sigma_{ij} + \Delta\sigma_{ij}) n_j \Delta u_{i,1} - \Delta\sigma_{ij} n_j u_{i,1}] \, d\Gamma \right\}. \tag{3b}$$

Here W is the stress work density, P is the kinetic energy density and m denotes the current number of time increments. The quantities n_i are the components of the vector normal to the contour Γ that surrounds the crack where it is assumed that the crack propagation is occurring in the x_1 direction.

A critically important aspect of eqn (3) is that its value is independent of the contour only in the limit as the contour shrinks onto the crack tip. Consequently, unlike the well-known J-integral for quasi-state crack growth based on deformation plasticity, the T^* parameter is path-independent only in a local sense. Application of the divergence theorem transforms the integral into a far field contour and a volume term which is more convenient from a computational viewpoint.

A number of important points need to be considered when T^* is computed that have a significant influence on the convergence of the parameter. For small scale yielding conditions, the stress singularity at the crack tip results in a finite value of T^* even when the inner contour is coincident with the crack tip. However, because of the weaker singularity in the vicinity of the crack tip for elastic–plastic materials, the T^* integral may vanish in the limit of mesh refinement. This does not occur if the appropriate definition of the elastic singularity in the region extremely close to the crack tip is achieved. Then, T^* will converge to a (small) finite number. Alternatively, an exclusion region can be introduced in the computation of the volume term. This is equivalent to taking the inner contour a small distance ε away from the crack tip. Frequently, this distance is the length of the smallest

element. This suggests that the T^* integral must be used in combination with some material-based length scale, e.g. by linking ε to some microstructural dimension of the material.

While parameters such as T^* are essentially energy based, geometric quantities have also been used to predict dynamic fracture. The most suitable has been the crack tip opening angle (CTOA). A relationship has been established between this quantity and T^* which is (Atluri, 1993)

$$T^* = k \in \sigma_{ult}(\text{CTOA}), \tag{4}$$

where σ_{ult} is the ultimate stress, ε is the size of the exclusion zone in the T^* computation and k is a dimensionless constant on the order of one. Thus, the CTOA can be viewed as an inelastic-dynamic generalization of K whereupon eqn (1) can be generalized to

$$\text{CTOA} = (\text{CTOA})_c, \tag{5}$$

where $(\text{CTOA})_c$ is the material property counterpart to K_D. Equation (5) is a plausible governing relation for dynamic crack propagation and arrest in ductile materials which has been used productively in the pipeline fracture propagation analyses described in the following section.

3. PIPELINE APPLICATIONS

While it is always desirable to prevent crack initiation, there are many occasions when this is not possible. This is particularly true when components are subjected to abnormal "third party" loads such as mechanical impact and near-by explosions. In these situations, it is then desirable that long running cracks be completely precluded by ensuring that crack arrest will take place. Until very recently a validated crack arrest methodology has not been used in the solution of practical problems. Recent work by the authors and their colleagues on pipelines, which is outlined in this section, illustrates the opportunities that exist in this important class of applications.

3.1. *Fluid/structure/fracture interaction*

A particularly challenging application of dynamic fracture mechanics technology has been to problems involving fluid/structure interaction. In this class of problems, the fluid pressures result in structural deformation in the containment boundary that in turn have the effect of modifying the fluid pressures. Thus, the behavior of a crack in such a component will be dependent on simultaneous and interactive changes in the structure and the fluid. The many examples in engineering where practical solutions are required for this problem category are typified by the fluid being contained by a thin cylindrical (shell) structure prior to rupture.

The authors and their colleagues (Kanninen *et al.*, 1989; O'Donoghue *et al.*, 1991) have developed a large scale computational analysis procedure for quantifying the interactive fluid/structure/fracture behavior of a fluid containment boundary perforated by a violent loading. The computational approach, embodied in an SwRI propietary computer program called PFRAC (pressure-boundary fracture analysis code), permits a fully coupled "first principles" analysis of the entire crack propagation event. Validation of this numerical approach has been provided by detailed comparison with full scale experiments on gas transmission pipelines (Kanninen *et al.*, 1992, 1993a). The primary features of the PFRAC code, which was used for the applications described in the following sections of this paper, are presented in Table 1.

3.2. *Large diameter, high pressure steel gas transmission pipelines*

Ductile fracture propagation in steel transmission pipelines has been the subject of much research by the gas industry (Kiefner *et al.*, 1973; Priest and Holmes, 1981; Venzi *et al.*, 1981; Holmes *et al.*, 1983; Ford, 1994; Eiber *et al.*, 1994). While early work focused on measures such as Charpy impact energy, for the inelastic dynamic material behavior

Table 1. SWRI integrated fluid structure fracture computational capability (PFRAC)

Structural mechanics unit	Fluid mechanics unit	Fracture mechanics unit
Dynamic finite element shell code	Three-dimensional finite difference code	Dynamic crack advance criterion
Elastic–plastic material behavior	Non-steady gas dynamics	Node release algorithms
Geometrically non-linear deformation	Two-phase flow behavior	Crack tip refinement via substructuring
Efficient explicit time integration	Moving obstacle feature	

that is observed during fracture of line pipe steel, recent work has shown that the CTOA is the most convenient crack tip characterizing parameter (Kanninen *et al.*, 1993a). To use this parameter to establish crack arrest conditions, it is only necessary to ensure that the maximum possible value of the "steady state" applied CTOA, which depends on pipe geometry and gas dynamics, is less than the critical material toughness value, labeled as $(\mathrm{CTOA})_c$. This follows from the highly plausible assumption that a long running fracture can only occur in a steady state condition. Accordingly, by quantifying the maximum steady state crack driving force, $(\mathrm{CTOA})_{max}$, that would occur with a given pipe geometry and initial gas pressure, it is then possible to specify the resistance required to preclude the steady state.

Based on eqn (5), a ductile fracture propagation event in a large diameter, high pressure, steel gas transmission pipeline is precluded provided that

$$(\mathrm{CTOA})_c > (\mathrm{CTOA})_{max}. \tag{6}$$

That a $(\mathrm{CTOA})_{max}$ occurs at some crack speed has been amply demonstrated by many computations and by theoretical considerations [see Kanninen and Popelar (1985)]. In essence, in a gas transmission pipeline, inertia forces increase inexorably with crack speed to the point where the crack driving force vanishes at a limiting steady state crack speed given approximately by

$$V_1 = \tfrac{3}{4} C_0 \left(\frac{h}{D}\right)^{1/2}, \tag{7}$$

where $C_0 = (E/\rho)^{1/2}$ is the bar wave speed, D is the pipe diameter, h is the pipe wall thickness and ρ is the density. The increase in crack driving force that arises from reduced gas decompression as crack speed increases then dictates that a maximum will exist. A typical PFRAC computational result is shown in Fig. 1.

This computational result can be compared with Fig. 2, which illustrates the deformation exhibited in a full scale pipe burst test conducted by Centro Sviluppo Materiali, Italy (Kanninen *et al.*, 1992), in a 1.42 m (56 in) diameter gas transmission pipeline. Figure

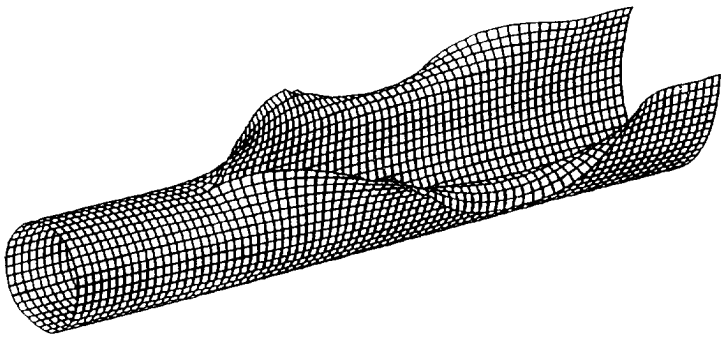

Fig. 1. Computational result for steady state crack propagation in a 1.42 m diameter steel gas transmission pipe pressurized to 100 bar.

1 shows the deformed shape of the pipe computed using PFRAC during steady state propagation in which it was assumed that the crack propagates in both directions from the symmetry plane at a constant speed of 125 m s^{-1}. This plot clearly illustrates the large deformation behind the crack tip that must take place if the end state revealed by Fig. 2 is to be achieved. In the pipe model, 1260 shell elements were used with the fluid being modeled by 14,560 cells. The computation time was of order 40 min on a CRAY 2 computer.

The $(CTOA)_{max}$ term of inequality (6) can be determined using PFRAC by calculating the steady state CTOA values for a range of different constant crack speeds. For each of a series of given pipe diameters, wall thicknesses, yield strengths and initial line pressures, several computations were performed over a range of constant crack speeds. These were carried out for methane, rich gas and wet gas. In each such analysis, a plateau value representing the steady state CTOA value for that particular constant crack speed was achieved. These steady state CTOA values were then plotted as a function of the hypothetical crack speeds. Of greatest utility is the fact that these plots show the existence of a maximum value at some particular crack speed. Results for 1.42 m (56 in) diameter pipes are shown in Fig. 3.

A procedure for the routine determination of the material toughness term $(CTOA)_c$ has become possible via a two-specimen test (Kanninen *et al.*, 1992). In this procedure two specimens, having distinctly different ligament dimensions, are broken using either a pendulum machine or a vertical drop weight machine with an instrumented hammer capable of recording the force–time variation during fracture. This record can then be integrated to give the force–deformation relation and hence the total energy to fracture. This total energy consists of an initiation portion and a propagation portion. With the two different ligament lengths, it is possible to extract the energy associated with the crack propagation and to relate it directly to the $(CTOA)_c$ value for that pipeline steel.

To validate the methodology, numerical simulations of full scale gas transmission pipe experiments were made using PFRAC to compute parameters that could be directly compared with measurements made in these tests. These simulations showed good agreement with the deformed pipe shapes, and with the axial and circumferential variations of the decompressed and decayed gas pressures accompanying ductile fracture propagation. Further, with the development of $(CTOA)_c$ data from the two-specimen procedure, the computed $(CTOA)_{max}$ values were used to delimit the propagate/arrest condition. This was followed by critical comparisons with the EPRG full scale test data base. A key step was to identify those few cases for which material property data and propagate/arrest results currently exist in order to make unequivocal critical comparisons. Only 15 data points were available. Most of these are for 1.42 m diameter pipes, but include a range of line pressures and grades of steel. The results are illustrated in Fig. 4, where it can be seen that the predictions are in perfect agreement with the arrest/propagate data. Because the PFRAC code is too cumbersome for routine use, to transfer the technology to pipeline engineers, a parametric study approach has been taken to determine $(CTOA)_{max}$ values. A broad range of pipe geometries, linepipe steels, gas pressures and gas compositions was analyzed. A dimensionless interpolating relation representing $(CTOA)_{max}$ was then taken in the form:

$$(CTOA)_{max} = C\left(\frac{\sigma_h}{E}\right)^m \left(\frac{\sigma_h}{\sigma_o}\right)^n \left(\frac{D}{h}\right)^q, \tag{8}$$

where σ_h is the hoop stress corresponding to the undisturbed line pressure, σ_o is the flow stress of the pipe steel, E is the elastic modulus of the pipe steel, D is the mean diameter of the pipe and h is the pipe wall thickness. Table 2 shows the computed values of C, m, n and q for the two bounding conditions associated with methane (or air) and a wet gas (Kanninen *et al.*, 1993a). Using eqn (8) and the two-specimen test procedure, determinations of the adequacy of a new pipeline design and of the critical pressure in an existing pipeline relative to fracture propagation can be readily made by gas industry engineers.

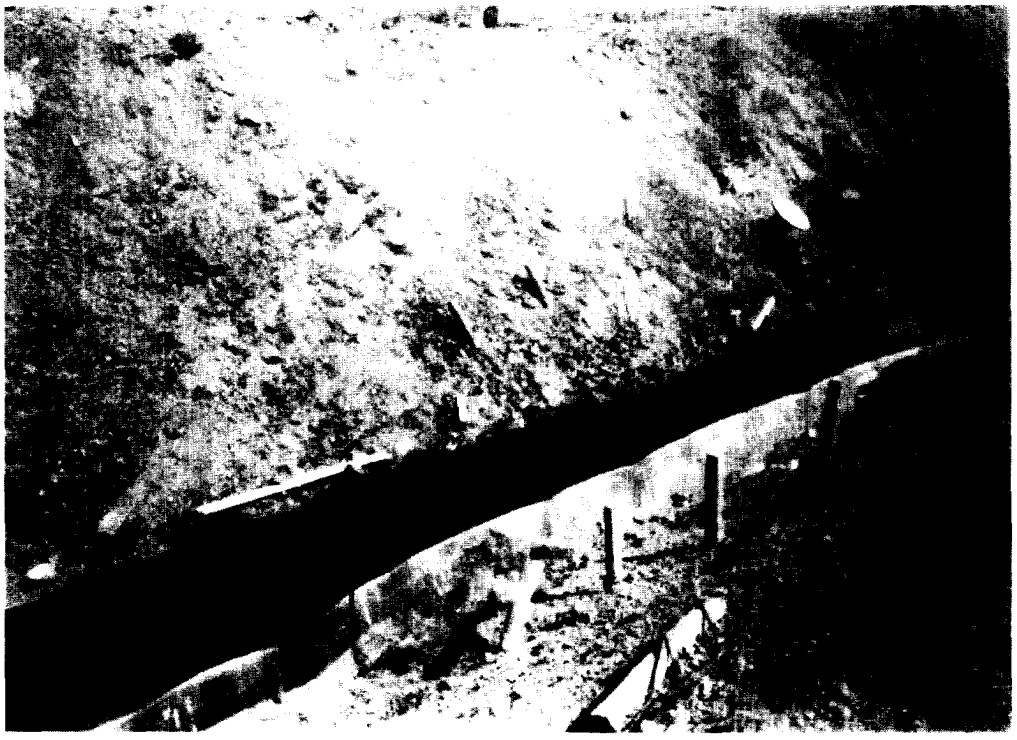

Fig. 2. Post-test photograph of a dynamic crack propagation experiment in a large diameter steel gas transmission pipeline.

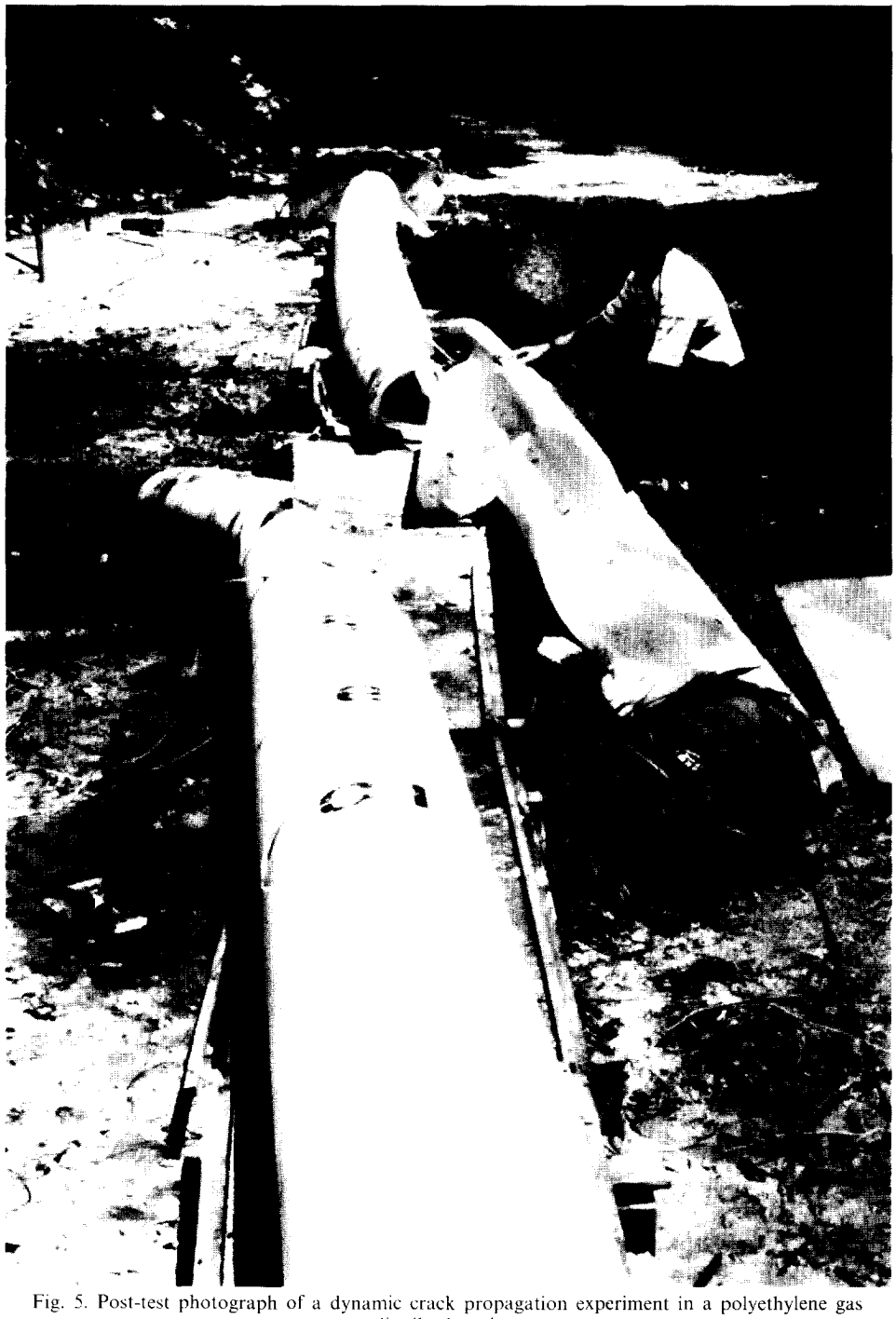

Fig. 5. Post-test photograph of a dynamic crack propagation experiment in a polyethylene gas distribution pipe.

Fig. 12. View of cracks emanating from a row of rivet holes—multi-site damage.

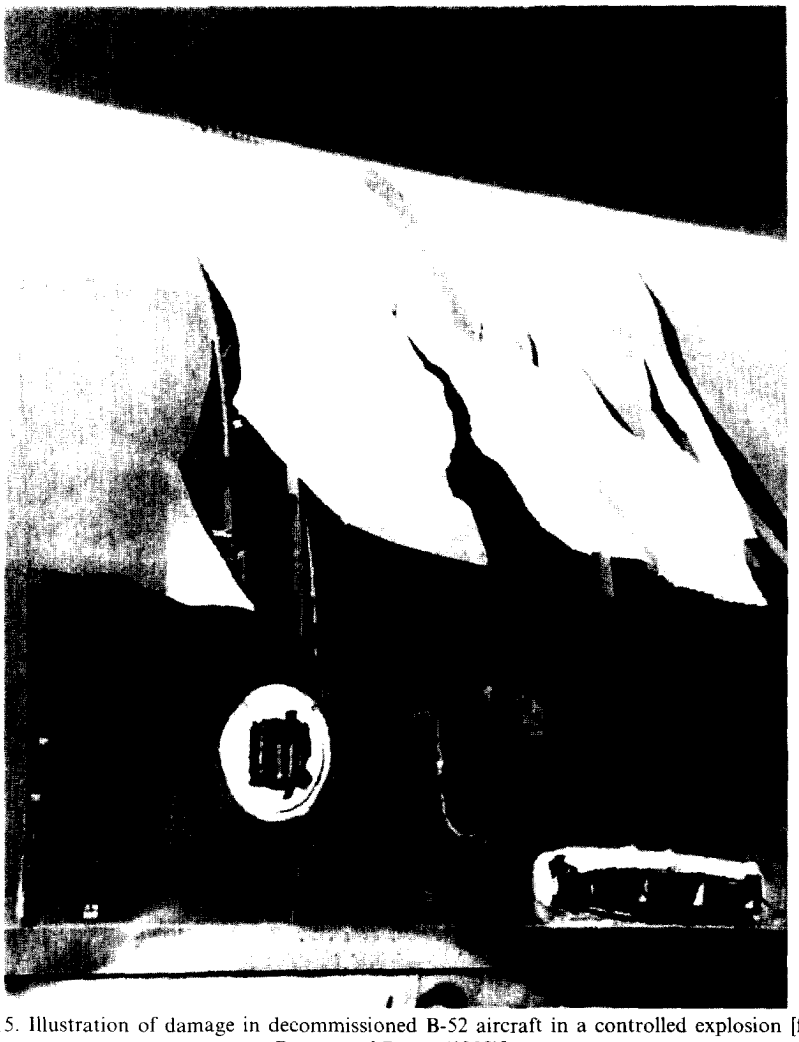

Fig. 15. Illustration of damage in decommissioned B-52 aircraft in a controlled explosion [from Barnes and Peters (1992)].

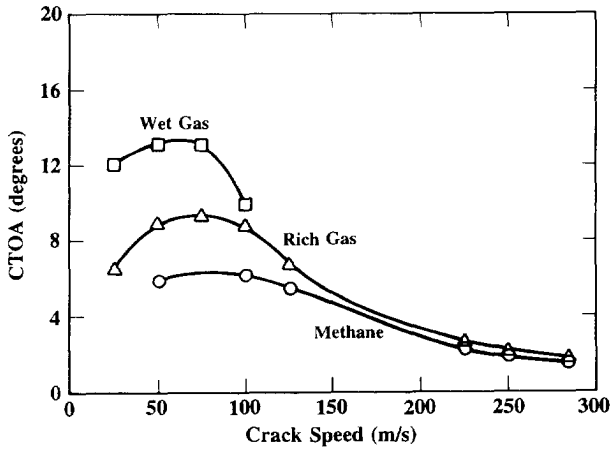

Fig. 3. Computational results for a 1.42 m diameter gas transmission pipeline showing the CTOA as a function of steady state crack speed for three different gas compositions.

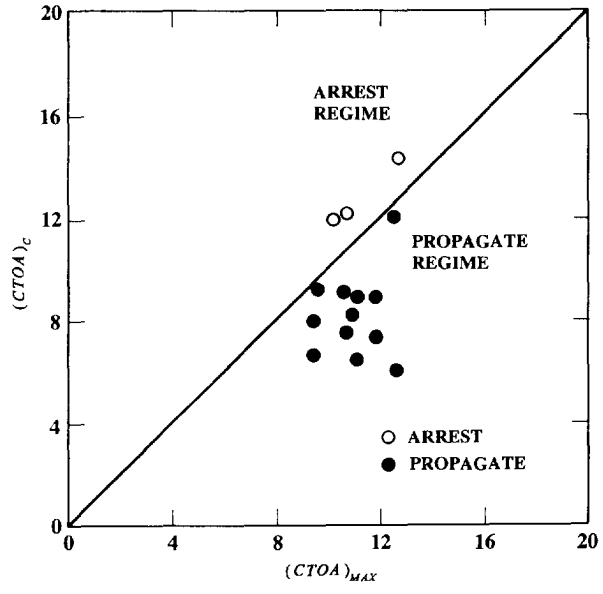

Fig. 4. Critical comparison of theoretical ductile fracture model propagate/arrest predictions with experimental results for 1.42 m diameter steel gas transmission pipes pressured by air.

Table 2. Values of dimensionless parameters in eqn (8)

Parameter	Lower bound (methane)	Upper bound (wet gas)
C	106	670
m	0.753	1.178
n	0.778	0.637
q	0.65	0.971

3.3. *Small diameter, low pressure polyethylene gas distribution pipelines*

Even though rapid crack propagation (RCP) in polyethylene (PE) gas distribution pipes has several similarities with the problem of ductile fracture in steel pipes, the material properties, geometry and loading are distinctly different. However, the objective of the work remains the same: to establish simple, reliable, readily-usable procedures for gas industry engineers to use in the design and operation of PE gas piping system to preclude large scale pipe rupture. Figure 5 shows the result of a full scale test conducted at SwRI

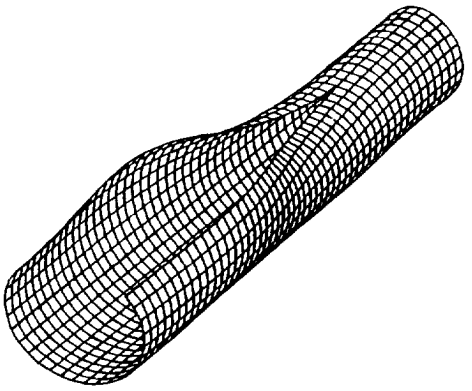

Fig. 6. Computational result for steady state crack propagation in a 400 mm diameter polyethylene gas distribution pipe pressurized by 6 bar.

illustrating that RCP is indeed possible. Also evident is the characteristic sinusoidal nature of the crack propagation and the closing of the crack due to the viscoelastic material behavior.

While the CTOA was used as the crack tip parameter for the steel pipe, because much smaller deformations are evidenced in the non-linear elastic behavior exhibited by PE, the energy release rate, G, is found to be more appropriate. A representative computational result for PE gas pipe using PFRAC, which can be contrasted with Fig. 1, is shown in Fig. 6. Note the reduced deformation in the case of the PE pipe due to the lower pressure and lower diameter-to-thickness ratio.

The determination of the dynamic crack driving force was accomplished with the PFRAC computer program using the rate-dependent non-linear elastic material behavior of the PE materials. These results exhibited a trend similar to that shown in Fig. 3, albeit only methane gas is of concern in gas distribution systems. By performing a large series of parametric computations, data enabling a formulation for the maximum RCP driving force can be expressed as

$$G_{\max} = \alpha p_L^{2.5} \frac{D}{E^{1.5}} (\text{SDR-1})^2, \tag{9}$$

where $G_{\max}$ is the maximum RCP driving force in kilojoules per square meter (analogous to the maximum CTOA of Fig. 3), p_L is the line pressure in bars, D is the mean pipe diameter in millimeters, E is the static elastic modulus in megapascals, α is a constant with a value of 0.0356 and SDR is the standard dimension ratio, the ratio between the outer pipe diameter and the wall thickness.

A complex dynamic fracture experiment known as the coupled pressure plate (CPP) technique was used to measure the dynamic fracture propagation toughness properties of PE gas pipe materials (Couque *et al.*, 1988). In this approach, a test specimen is loaded very rapidly to promote a constant crack velocity that is characteristic of the actual pipe rupture event. Through a finite element simulation of the test, the technique provides the dynamic fracture toughness (denoted G_D) as a function of the test temperature and the wall thickness. However, while precise G_D values can be determined for all materials, there are too many different PE materials and operating techniques to make the use of the complex CPP technique practical. Accordingly, on the assumption that in PE gas pipe materials the RCP initiation energy is negligible compared with the propagation energy, an empirical approach was adopted in which Charpy impact energy values were used to index the CPP data. The correlation of dynamic toughness to Charpy energy for two medium density PE (MDPE) materials was found to be (Kanninen *et al.*, 1993b)

$$G_D = 1.62 C_v, \tag{10}$$

where C_v denotes the absorbed energy per unit area in a Charpy impact test. While the

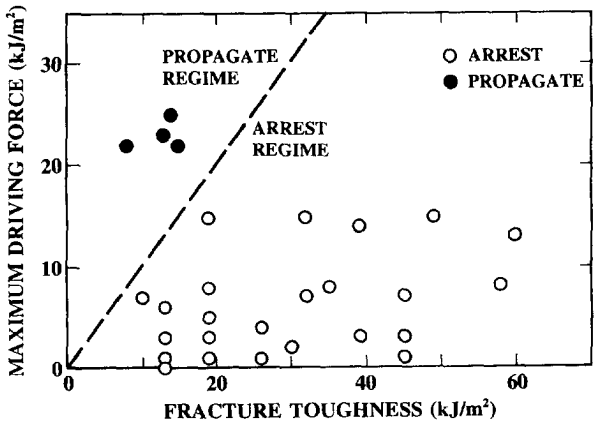

Fig. 7. Validation of rupture guidelines by the successful prediction of pipe rupture and arrest in tests conducted by SWRI, Battelle, British Gas and Dupont.

number of CPP data available was not overly large, it is believed that eqn (10) is reasonably representative of medium density PE materials. A validation of the methodology is provided by the results shown in Fig. 7.

Each of the data points in Fig. 7 corresponds to a full scale test carried out by one of four separate industrial concerns that represented a broad range of pipe sizes and operating conditions. For each test, the dynamic fracture toughness was calculated using eqn (10) with the driving force calculated using eqn (9). In four instances long running cracks were observed (designated as PROPAGATE), with crack arrest occurring soon after initiation in the remainder (designated as ARREST). It can be seen that, by using the methodology described herein, correct predictions were made in all instances.

As a further illustration of the validity of the analysis methodology, a set of computations was performed for a 250 mm diameter SDR 17.6 MDPE gas pipe pressurized by air at pressures of 6.1 and 7.1 bar, conditions that correspond to the full scale experiments conducted by Grieg (1985). The computed G values for steady state RCP attained over a range of hypothetical crack speed values at each pressure are shown in Fig. 8. It can be seen that a "dome shaped" curve results when the crack driving force is plotted as a function of hypothetical crack speed with a maximum value being clearly identifiable for each pressure. These data provide a basis for an independent comparison with the test data, as follows. Because the critical pressure determined by Grieg was 6.1 bar, the maximum of the crack driving force curve computed for that pressure must, in principle, correspond to the toughness of this material. As indicated by the horizontal line in Fig. 8, this value is $G_c = 30$ kJ m^{-2}. Now, it can also be seen from Fig. 8 that the horizontal line intercepts the

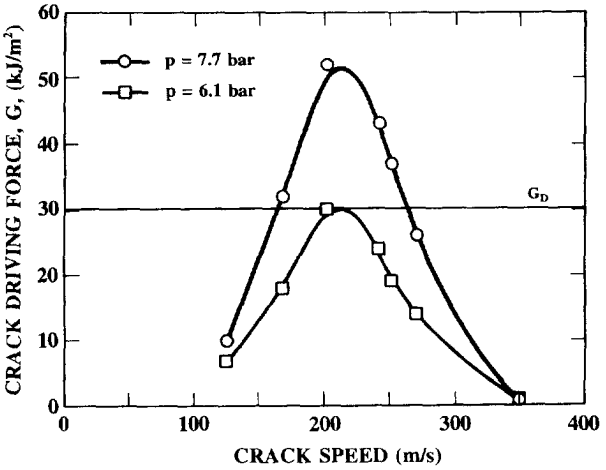

Fig. 8. Computed RCP driving forces as a function of postulated crack speed for a 150 mm diameter SDR 17.6 MDPE gas pipe at two different pressures.

7.1 bar pressure curve at two crack speeds: 160 and 260 m s^{-1}. Quoting from the description of these tests given by Grieg (1985):

> The crack ran consistently at the decompression speed for 10.5 m then dropped to 167 m s before increasing to a reasonably steady 270 m/s. Surprisingly, the crack appeared to be able to run in a stable manner at *two* speeds.

Not only is the type of result exhibited by the model the only plausible form that can accommodate stable RCP at two speeds, it can be seen in Fig. 8 that the speeds that are predicted are in very close agreement with the observed values. In addition, a stability argument given by Kanninen and Popelar (1985) explains why the change from one ostensibly stable state to the other must be from the lower speed to the higher speed. This is also consistent with the results given in the above quotation.

The technology can readily be used by industry by writing the combination of eqns (9) and (10) in different ways. The most descriptive relation is one that determines the minimum Charpy energy that a material must have in order to preclude pipe rupture. In the units of eqn (9), this relation is

$$(C_v)_{\min} = 0.022 p_L^{2.5} \frac{D}{E^{1.5}} (\text{SDR-1})^2. \tag{11}$$

A corresponding expression can readily be obtained for application to an existing pipeline to determine a maximum pressure that can mitigate RCP.

Future work in this area will focus on replacing the Charpy energy as the measure of RCP resistance. This test is currently used in the rupture prevention procedure primarily because it can be readily performed by the gas industry. However, it is recognized that the Charpy energy is a highly approximate measure of PE resin toughness (in the sense used in the procedures described herein), as previously recognized in work on gas transmission pipelines—see Section 3.2. The major shortcoming of the Charpy energy is that it combines the energy required to initiate fracture with the propagation energy. A second shortcoming unique to polymeric pipe materials is that, because the Charpy specimen is cut from the pipe wall, thickness effects and residual stress effects, which are known to influence RCP, are ignored. Accordingly, work is in progress to develop an improved rupture prevention procedure based on the likely ISO RCP standard—the small scale steady state (S4) test apparatus developed by Yayla and Leevers (1989).

The S4 test captures the influences of pipe wall thickness and residual stress. However, as it is currently used, several tests are needed to determine the critical pressure for RCP; a result that is not firmly connected to the in-service critical pressure. By integrating the S4 test with a computer code like PFRAC, these shortcomings can be overcome. In principle, provided the pressure is high enough that crack propagation through the pipe section is ensured, only one S4 test needs to be conducted. Using the crack history measured during the test, PFRAC can be used to simulate the S4 test, including the effects of the internal baffles of the S4 rig. From the computational results, the dynamic toughness of the particular PE resin at the test temperature can be inferred. This new toughness measure can then be directly inserted into eqn (9), obviating the need for eqn (6).

4. AEROSPACE APPLICATIONS

The preceding section of this paper described dynamic fracture applications to gas transmission and distribution pipelines, areas in which work has been carried to the point where the industry can make practical use of the results. In contrast to the gas industry where the need for this type of technology has long been evident, aerospace interest in dynamic fracture mechanics is of much more recent origin. This section outlines some preliminary applications that, while not complete, will serve to provide further illustration of the potential of dynamic fracture mechanics for resolving engineering problems of high practical interest.

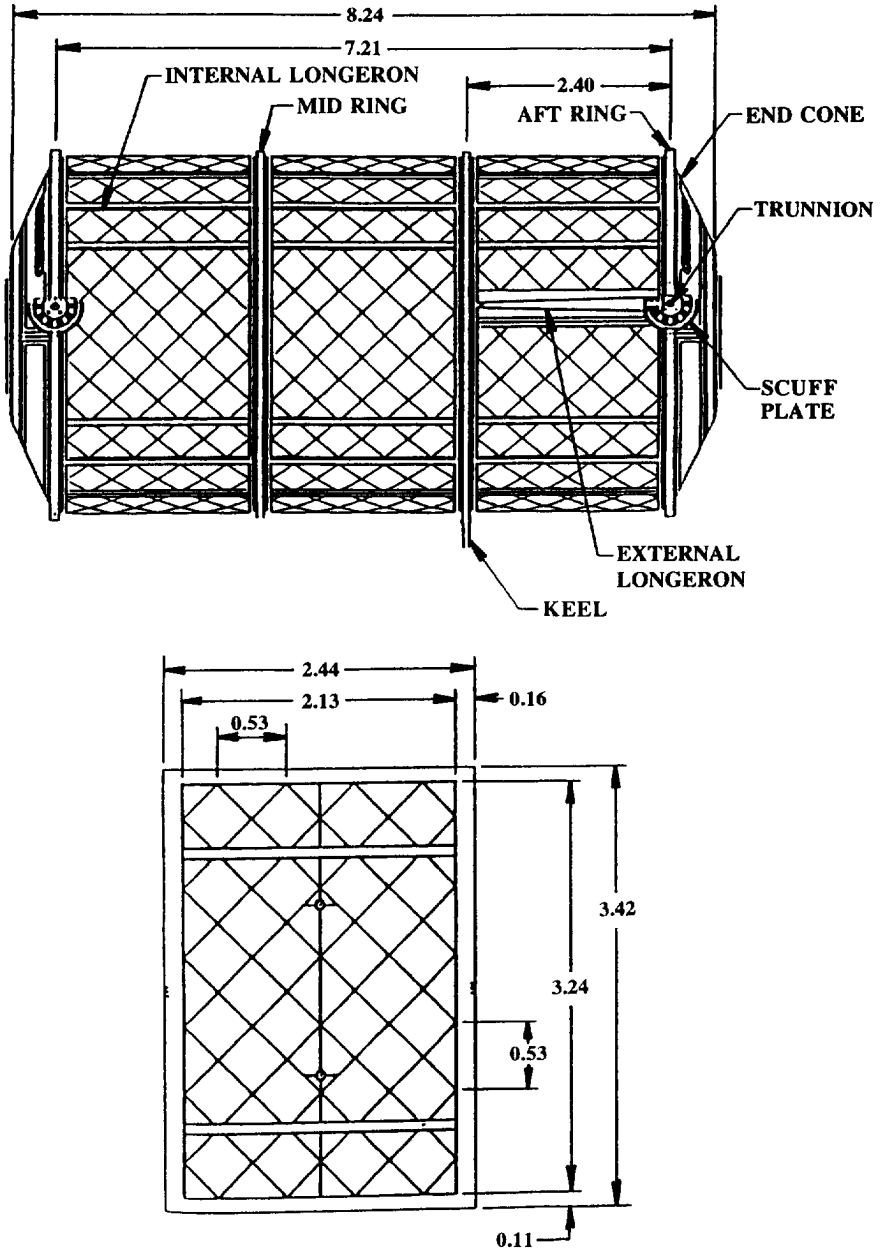

Fig. 9. Schematic view of inhabited space station module.

4.1. *Orbital debris impact on space station modules*

A major portion of the critical items envisioned for the space station are pressure vessels, ranging from the inhabited and laboratory modules to high pressure fuel tanks. A schematic of the Space Station Freedom (SSF) module is shown in Fig. 9 (dimensions in meters). A key element of the design is concern for impact by micrometeroids or orbital debris (M/OD). Because of the large density of M/OD, it is necessary to ensure that these pressure vessels will not fail catastrophically when subjected to the impulsive load (typically only of the order of 10 μs duration) of M/OD impact. If sufficiently large, such impacts could puncture the vessel wall in a violent manner, typically producing several relatively large petals. The torn material between the petals could act as initiation sites for catastrophic fracture propagation.

Due to the rapid loading, the petals would be formed very quickly, i.e. in the order of 10–100 μs. Thus, if the crack propagates from the initiation site at or shortly after impact, it would be a dynamic event. To quantify the potential for unzipping failure of the SSF

pressure vessels, a number of fracture mechanics analyses were carried out for the inhabited module geometry subjected to M/OD perforation. This work was complemented by the experimental determination of static and dynamic plasticity and plane stress fracture properties for the relevant aluminum alloy. The results were used to obtain an estimate of the critical crack size at which continued crack propagation would take place (Couque *et al.*, 1993).

An initial estimate developed by the space station design team using a static linear elastic fracture mechanics approach led to a solution that was extremely conservative. This procedure was based on the stress intensity factor relation for a relatively small axial crack in a pressurized cylinder that accounts for the outward bulging of the wall in the vicinity of the crack. Separate relations have been developed by Folias (1965) and Erdogan and Kibler (1909). These can be written in the common form

$$K = \sigma_h(\pi a)^{1/2}\left[1+\alpha\frac{a^2}{Rh}\right]^{1/2}, \tag{12}$$

where K is the stress intensity factor (crack driving force), $2a$ is the crack length, σ_h is the hoop stress, R and h are the vessel mean radius and wall thicknesses, respectively, while α is a dimensionless constant that is equal to 1.61 in Folias's result and equal to 1.25 in Erdogan and Kibler's result. Use was made of eqn (12) by finding the initial crack length such that K is equal to 55 MPa $m^{1/2}$, which is a conservative estimate of K_c for the 3.17 mm thick 2219-T87 aluminum alloy proposed for SSF pressure. This produces a critical crack size of 0.15 m.

The dynamic fracture mechanics approach of Couque *et al.* (1993) combined PFRAC analyses with dynamic fracture experimentation. First, dynamic R-curve data for the 3.17 mm thick 2219-T87 aluminum alloy were developed. Figure 10 shows that the dynamic R-curve is significantly higher than the quasi-static R-curve for a 3.17 mm wall thickness. Next, PFRAC was used to compute crack driving forces consistent with a dynamic input that creates a large jagged hole. The crack size that corresponds to the tangency point can be determined that will delineate the boundary of unstable growth, i.e. if larger crack sizes are created by the impact, they will unzip. The result is a critical crack length of 1.0 m. Figure 11 shows the inelastic-dynamic crack driving forces for wall thickness of 3.17 and 4.83 mm that were used with Fig. 10 to determine this result.

A dynamic fracture propagation analysis using PFRAC has also been used to investigate crack propagation in the pressurized modules. As input to the code, the fracture toughness was specified as a function of crack velocity (as determined from experimental data). In each analysis, an initial crack length was specified and propagation assumed to take place in accordance with the fracture toughness relation. Crack arrest is predicted when the driving force drops below the minimum toughness. The objective was to find the initial crack length for which there was continued crack propagation with no arrest. This

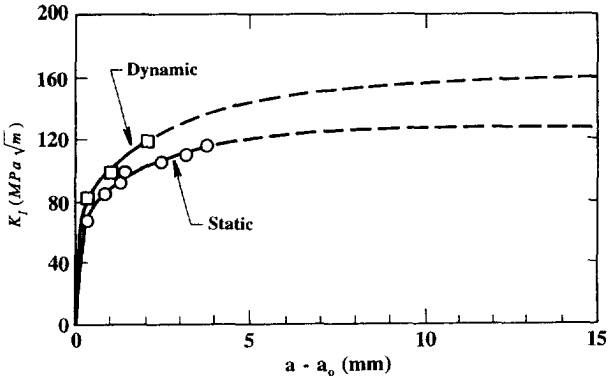

Fig. 10. Quasi-static and dynamic R-curves for the 3.17 mm thick Al2219-T87 CCP specimen.

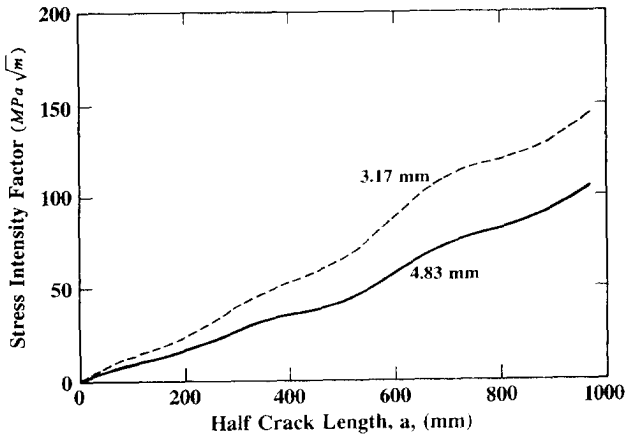

Fig. 11. Computed stress intensity factors as a function of crack length for two thicknesses of Al 2219-T87 for the inhabitated module geometry.

was found to be considerably longer than the lengths calculated using the R-curve approach, indicating its conservative nature.

4.2. *Multiple site damage in an aircraft fuselage*

The possibility of large scale catastrophic crack propagation in an aircraft first came to light in connection with the de Havilland Comet accidents in 1954 (Swift, 1987). More recently, there have been a number of instances of fuselage failure resulting from crack initiation in the vicinity of rivet holes. The best known example of this was the Aloha airlines incident in 1988 (Hendricks, 1990) where it was found that many short cracks can exist in a row of riveted lap splice joints; see Fig. 12. The presence of multiple cracks at rivet holes or elsewhere in a single component is referred to as multiple site damage (MSD). MSD cracks can grow under fatigue loading and can eventually link up. Clearly this is an undesirable situation but one that will not be fatal provided any cracks that propagate quickly arrest. This is conventionally achieved with the aid of "tear straps", a rectangular grid that is bonded to the inner surface of the fuselage (Shimamoto *et al.*, 1994). Provided these straps prevent continued propagation of the crack, safe decompression will occur.

As the link-up process takes place, the configuration can be viewed as a long crack in a thin pressurized cylinder. Analysis of this situation presents a number of interesting technical challenges including the quantification of bulging in the vicinity of the crack, the possibility of dynamic effects due to local instabilities, and the estimation of air leakage through the opened crack. To examine these items, a computational capability such as PFRAC is required. To assess the suitability of this code to quantify the importance of the various nonlinear effects, an analysis was developed for a Boeing 737 aircraft with material properties of 2024-T3 aluminum (Kanninen *et al.*, 1991).

As the first step, a computation was made to determine the local bulging of the skin due to an axial crack in an unreinforced fuselage. In the analysis, the skin was simply treated as a thin circular cylindrical shell. Figure 13 shows pseudo stress intensity factor values computed for a range of axial crack lengths for unreinforced skins. The definition $K=(EG)^{1/2}$ has been used for convenience where E denotes the elastic modulus and G is a measure of the elastic–plastic crack driving force.

Computational results like those in Fig. 13 are meaningful only in relative terms. While one benchmark is the fracture toughness, these values can vary over a wide range. NB, for 2024-T3 aluminum, K_c ranges from 80 up to 160 MPa $m^{1/2}$. Another basis of comparison would be "standard" LEFM expressions for the stress intensity factor. The most suitable is the relation for a pressurized cylinder given by eqn (11). The second reference solution is for a crack in a flat plate under in-plane loading. From Fig. 13, it can clearly be seen that the computed solutions differ markedly from these two reference cases. Of greater importance, a distinct difference can be seen between the geometrically non-linear elastic solution and the elastic–plastic geometrically non-linear solutions obtained from the

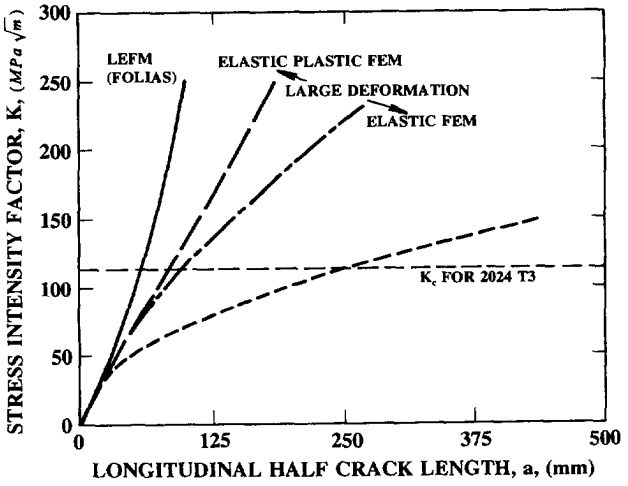

Fig. 13. Comparison of computed stress intensity factors for different geometric and material behavior modeling assumptions.

enhanced PFRAC code. Because the neglect of elastic–plastic behavior is anti-conservative, it would appear that the geometrically non-linear elastic–plastic approach should be adopted for the consideration of long cracks (i.e. crack lengths greater than the tear strap spacing) in fuselage structures.

On the basis of the results shown in Fig. 13, it is evident that elastic–plastic deformation can be significant for long cracks in thin-skin aluminum 2024-T3 materials. Accordingly, further computations were carried out to examine the effect of airframe stiffeners using this approach. The preliminary results indicate that this mode of reinforcement provides only a modest reduction in the stress intensity factor, probably because it is the non-linear material behavior that dominates. In general, the tear strap causes the crack to turn and propagate circumferentially—a complicated process in view of the associated curved crack propagation (Shimamoto *et al.*, 1994).

The process through which cracks at near-by rivet holes link-up to form a large crack is one to which dynamic effects contribute. In particular, because inertia effects generally act to enhance the stress state while rapid motion tends to reduce the resistance of the material to crack advance, the neglect of dynamic effects could be anti-conservative (Swift, 1992). Rather than attempt to simulate actual aircraft fuselage geometries, some relatively simple computations were performed for a preliminary assessment of the dynamic enhancement of the crack driving forces resulting from the rapid link-up of MSD sites. As expected, the higher the crack speed, the greater the dynamic crack driving force. For example, in a two-dimensional planar calculation a 25% enhancement was noted at a crack velocity of 125 m s^{-1}. While this dynamic amplification of the driving force is not large, an additional consideration is that the dynamic fracture propagation toughness values are also greater than the static initiation toughness values.

4.3. *Blast loading in aircraft*

The drastic consequences of terrorist-induced blast loading in a commercial aircraft were highlighted by the Lockerbie tragedy in 1989 when a Pan Am aircraft was destroyed with enormous loss of life (U.K. Air Accidents Investigation Branch, 1990). A schematic view of the damage from this incident is shown in Fig. 14. This event has promoted a review of blast protection measures on aircraft (Report of the President's Commission, 1990). While detection procedures will always ensure that the quantities of explosive will not be very large, small amounts of explosive can still have devastating effects. It is desirable to quantify these effects and to establish if remedial action can in some manner increase the chances of aircraft survivability. For example, consideration has been given to venting the explosive through designated panels to ensure safe decompression, a procedure misleadingly called "aircraft hardening".

Table 3. Blast loading regimes for aircraft explosions

Regime	Characterization	Time scale (ms)	Analysis methodology
1	Explosive detonation	0–0.2	Hydrocode
2	Blast wave propagation through surroundings to fuselage	0.2–0.5	Hydrocode
3	On-set of structural deformation and damage	0.5–5	Hydrocode
4	Large scale damage propagation by crack growth initiation and fast fracture with fluid–structure interaction	5–100	Coupled structural and fluid mechanics codes

During an explosive event on an aircraft, there are a number of different processes that take place, and these take place at different times after the detonation of the explosive. These four regimes are summarized in Table 3. From the numerical simulation viewpoint, a hydrocode is required to simulate the initial detonation and subsequent base wave propagation. However, once the wave impinges on the fuselage, it will be more convenient to use a structural analysis code. In this sense, PFRAC is ideally suited particularly as it allows simulation of any fast fracture of the fuselage skin.

Test data generated by the U.S. Air Force on decommissioned B-52 aircraft on behalf of the Federal Aviation Administration have been used to investigate the effects of blast loading. One charge was used in each test, but these charges had different masses and were placed at different locations. In all, five tests were conducted and the damage in each case was quantified. These tests were also instrumented with accelerometers and strain gages. The fuselage pressures were calculated using the BLASTIN code. This empirically based code was used as an expedient in place of a full hydrocode analysis of the charge detonation and blast propagation. This approach was vindicated by the good correlation of the B-52 experimental results and the BLASTIN data that was established.

A triangular pressure distribution was calculated for each PFRAC element based on time of arrival, the peak pressure and the pulse duration. Blast wave reflections and other interactions that were considered to be secondary events were not included. Using these loadings, PFRAC calculations were carried out and the results monitored at the location of maximum damage, as observed experimentally. In particular, the equivalent plastic strain was calculated as a measure of the on-set of damage. These results are summarized in Table 4. The tests are listed in ascending order of damage as observed experimentally. It can be seen that the computational results correlate very well with these data. Figure 15 illustrates the damage observed in tests E (Barnes and Peter, 1992).

5. RESEARCH CHALLENGES

As the preceding sections were intended to show, dynamic fracture mechanics has evolved and matured to the point where results of practical interest can be obtained. Nonetheless, a significant number of issues remain to be resolved that present barriers to

Table 4. Comparison of dynamic fracture analyses with experimental bomb blast data for retired B-52 aircraft

Test number	Charge designation†	Experimentally observed damage‡	Computed results: equivalent plastic strain
9205	A	Minor internal damage	0.58×10^{-2}
9213	B	Increased internal damage	2.89×10^{-2}
9207	C	Popped rivets (4 frames)	3.06×10^{-2}
9217	D	10 in crack	4.49×10^{-2}
9212	E	Extensive cracking (10 ft)	5.55×10^{-2}

† Letters denote charge size with A being the lowest and E the highest.
‡ Tests are listed in ascending order of potential for damage from the given.

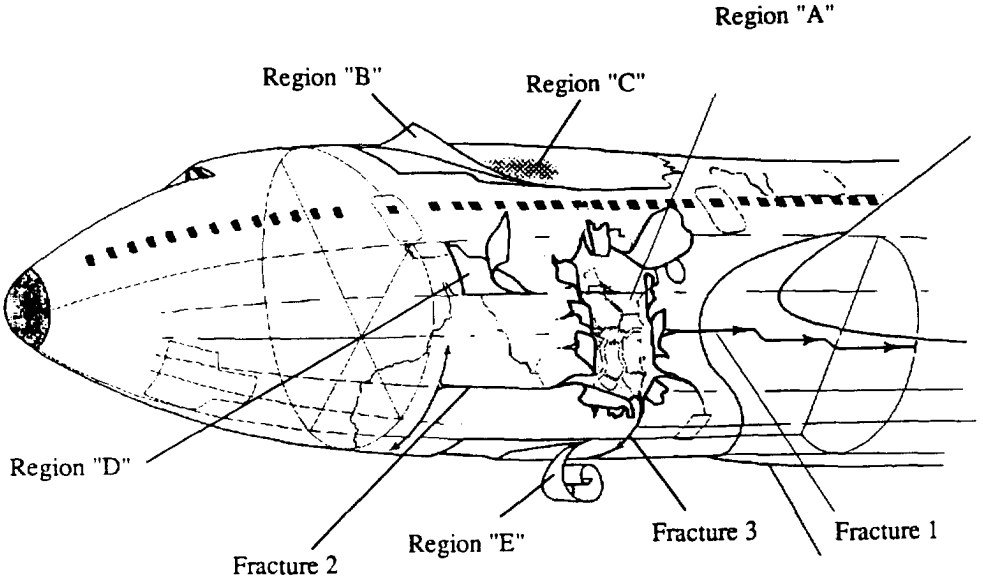

Fig. 14. Schematic view of explosive damage in Pan Am aircraft [from U.K. Air Accidents Investigation Branch (1990)].

further dynamic fracture mechanics applications. Some selected research challenges are as follows.

5.1. *Crack formation*

The "missing link" between applied mechanics and fracture mechanics is at the transition from a highly deformed continuum to a body with a crack-like penetration or perforation. From a very basic point of view, an instantaneous quantity such as equivalent plastic strain can be used as an indication of the location of potential damage or failure. A more pragmatic approach is to use a cumulative damage measure. In either case, of note is the fact that such an approach can at best determine where and when a crack could be formed, but cannot quantify the size, shape or the orientation of such a crack.

High velocity projectile impact and explosive blast represent another loading regime that induces complex failure processes. While much research has been devoted to these issues (Anderson, 1993), and indeed successful predictions of deformation/damage have been made in many instances, there are a number of fundamental problems that must be solved. During perforation of a component such as a thin pressurized cylinder, a number of clearly defined cracks will often emanate from the breach. The prediction of the number, size and orientation of these cracks represents a big challenge to the research community. In addition, it sometimes happens that one of these cracks becomes dominant and propagates the entire length of the component resulting in a catastrophic failure. An example of this problem is the debris impact of a space station that is discussed above.

Complicating these failure processes is the fact that shock waves are dominant at early times, but begin to dissipate at later times as the fracture event takes place. Fragmentation, resulting from impact or some other form of shock loading, represents another complex process during material failure. This is essentially equivalent to multiple crack initiation and simultaneous propagation. This phenomenon remains to be rigorously quantified.

5.2. *Dynamic viscoplasticity*

Materials such as nuclear reactor pressure vessel and gas/oil transmission pipeline steels exhibit viscoplastic behavior in the vicinity of a propagating crack. This has proved difficult to characterize, particularly in view of the ultra-high strain rates that are experienced during propagation. Clearly, linear elastic quantities such as the stress intensity factor are invalid in the absence of small scale yielding. While a number of viscoplasticity models are available (Bodner and Partom, 1974), because the nature of the singularity at the crack tip

has been difficult to establish, as discussed earlier, no single, physically meaningful, inelastic-dynamic crack tip dominating parameter has been identified to provide the basis for developing crack propagation/arrest procedures (Dexter and O'Donoghue, 1993). Laboratory testing to determine the characteristic fracture parameter (Kanninen *et al.*, 1990) is certainly non-trivial and doubts exist as to the uniqueness of the relationship of such a quantity to the crack velocity. Consequently, the transferability of the crack tip parameter from one geometry to another is not possible at present.

5.3. *Crack propagation curving and branching criteria*

For conditions in which small scale yielding occurs, the linear elastic fracture mechanics parameter K, the stress intensity factor, dominates the near crack tip region. It can then be expected that eqn (3) will govern dynamic crack initiation, propagation, arrest and reinitiation. However, when the zone of plastic deformation in a metal (or crazing in a polymer) that attends the crack tip becomes too large, non-linear parameters are needed. Many have been offered and used successfully including the CTOA and contour/area integrals such as T^*. Notwithstanding the successes that have been achieved, the establishment of a generally applicable inelastic-dynamic crack tip parameter, having a firm theoretical basis and a clear procedure for establishing its critical values as material properties, is a needed basic element.

It frequently happens that a propagating crack does not travel in a straight line. This is not surprising in the case of mixed mode loading, but it has also been observed when mode I loading conditions ostensibly dominate. An example of the latter is the sinusoidal nature of crack propagation that has been observed in gas pipelines; see Fig. 5. Note that, while the test result shown in Fig. 5 is on a polymeric pipe material, very similar behavior occurs in steel pipes. While crack curving, crack branching and ring off have been investigated [see, for example, Erdogan and Sih (1963); Hussain *et al.* (1974); Sih (1974); Streit and Finni (1980)], they still represent challenging issues for the fracture community. A worthy challenge is to develop a complete and rigorous model that could predict the crack path shown in Fig. 5.

5.4. *Applications to inhomogeneous media*

In recent years, there has been a tremendous increase in the use of fiber-reinforced composites, ceramics and other advanced materials for engineering components and structures in the aerospace and other industries. While fracture mechanics methodologies are well developed for metals that are homogenous and isotropic, the complex behavior of the new materials is not fully quantifiable. In many instances, a single dominant through-thickness crack is not present. Frequently, there is evolution of some damage that eventually leads to failure of the component. For example, the progression of damage in a fiber-reinforced composite from matrix cracking to delamination to fiber breakage involves the combination of several mechanisms. The interactions between the stiff fiber and the relatively compliant matrix play an important role in this failure process. Because many advanced materials are particularly vulnerable to dynamic loadings, there is an obvious need to develop procedures to characterize dynamic damage and fracture for inhomogeneous materials that can be used on a routine basis to assess the integrity of the components.

5.5. *Residual stresses*

Residual stresses frequently arise during the differential cooling that occurs during component manufacture and, in particular, in joining operations. Residual stresses are usually self-equilibrating and can either promote or retard growth depending on whether the stress fields are tensile or compressive in the vicinity of a crack tip. The influence of these residual stresses on crack growth has been difficult to quantify because they are strain controlled, and hence change during the crack growth process. A further complexity arises in welding where metallurgical changes can occur due to high rates of heating and can change the material resistance to crack growth.

6. CONCLUDING REMARKS

Selected applications of dynamic fracture mechanics to pipelines and aerospace vehicles are reviewed in this paper, both to demonstrate the utility of the technology and to show that basic issues can and do arise from practical applications. The writers hope that these selections will challenge and stimulate the research community to be concerned with dynamic failure. They further hope that researchers will also come to appreciate better the usefulness and appropriateness of more directly connecting basic research to applications.

Acknowledgements—The research described in this paper touched on work performed in internal research at the Southwest Research Institute along with work conducted in SwRI projects sponsored by the Gas Research Institute, the A.G.A. Pipeline Research Committee, the Federal Aviation Administration and Grumman Space Station Integration Division.

REFERENCES

Anderson, C. E. (Guest editor) (1993). Proceedings of the Hypervelocity Impact Symposium, San Antonio, Texas. *Int. J. Impact Engng* **14,** Nos 1–4.

Atluri, S. N. (1982). Path independent integrals in finite elasticity and inelasticity with body forces, inertia and arbitrary crack face conditions. *Engng Fracture Mech.* **16,** 341–364.

Atluri, S. N. (1993). Private communication to M.F. Kanninen.

Barnes, J. and Peters, R.L. (1992). The challenge of commercial aircraft survivability. In *Aerospace America*, pp. 55–56.

Bodner, S. R. and Partom, Y. (1974). Constitutive equations for elastic viscoplastic strain hardening materials. *J. Appl. Mech.* **42,** 385–389.

Brust, F. W., Nishioka, T., Atluri, S. N. and Nakagaki, M. (1985). Further studies on elastic plastic stable fracture utilizing the T^* integral. *Engng Fracture Mech.* **22,** 1079–1104.

Couque, H., Hudak, S. J. and Lindholm, U. S. (1988). On the use of coupled pressure bars to measure the dynamic fracture initiation and crack propagation toughness of pressure vessel steels. *J. Phys. Supplement*, Supplement No. 9, T49, pp. C347–C352.

Couque, H., O'Donoghue, P. E., Mullin, S. A. and Kanninen, M. F. (1993). Investigation of crack initiation and unstable propagation due to meteoroid or orbital debris impact into space station freedom pressure vessels. Southwest Research Institute Report to Grumman Space Station Integration Division.

Dexter, R. J. and O'Donoghue, P. E. (1993). Computational procedures and energy integral for dynamic fracture in viscoplastic material. *Engng Fracture Mech.* **44,** 591–607.

Eiber, R. J., Bubenik, T. A. and Leis, B. N. (1994). Pipeline failure mechanisms and characteristics of the resulting defects. In *Energy Transportation, Transfer and Storage Conference*, pp. 25–27. Pennwell, Houston, Texas.

Ensley, J. (1994). Energy and Fuels. *New Scientist*. Inside Science Number 68, 15 January.

Erdogan, F. and Kibler, J. J. (1969). Cylindrical and spherical shells with cracks. *Int. J. Fracture* **5,** 229–237.

Erdogan, F. and Sih, G.C. (1963). On the crack extension in plates under plane loading and transverse shear. *ASME J. Basic Engng* **85,** 519–527.

Folias, E. S. (1965). An axial crack in a pressurized cylindrical shell. *Int. J. Fracture* **1,** 104–114.

Ford, I. J. (1994). Rupture of pressurized tubes by multiple cracking and fragmentation. *Int. J. Pressure Vessels Piping* **57,** 21–29.

Freund, L. B. (1990). *Dynamic Fracture Mechanics*. Cambridge University Press, Cambridge.

Grieg, J. M. (1985). Fracture propagation in 250 mm and 315 mm polyethylene gas pipes. British Gas Engineering Research Station Report E472.

Gurney, R. W. (1943). The initial velocities of fragments from bombs, shell and grenades. U.S. Army Ballistic Laboratory, BRL Report 405.

Hendricks, W. R. (1990). The Aloha Airlines accident—a new era for aging aircraft. In *Structural Integrity of Aging Airplanes* (Edited by S.N. Atluri, S.G. Sampath and P. Tong), pp. 153–166. Springer, Berlin.

Holmes, B., Priest, A. H. and Walker, F. E. (1983). Prediction of linepipe fracture behavior from laboratory tests. *Int. J. Pressure Vessels Piping* **12,** 1–27.

Hussain, M. A., Pu, S. L. and Underwood, J. H. (1974). Strain energy release rate for a crack under combined mode I and mode II. *Fracture Analysis*, ASTP STP **560,** 2–28.

Kanninen, M. F. and Atluri, S. N. (Editors) (1986). *Dynamic Fracture Mechanics*. Pergamon Press, New York.

Kanninen, M. F. and Popelar, C. H. (1985). *Advanced Fracture Mechanics*. Oxford University Press, New York.

Kanninen, M. F., O'Donoghue, P. E., Green, S. A. and Morrow, T. B. (1989). The development and verification of dynamic fracture analysis procedures for flawed fluid containment boundaries. Southwest Research Institute IR&D Report, San Antonio, Texas.

Kanninen, M. F., Hudak, S. J., Couque, H. R., Dexter, R. J. and O'Donoghue, P. E. (1990). Viscoplastic-dynamic crack propagation: experimental and analysis research for crack arrest applications in engineering structures. *Int. J. Fracture* **42,** 239–260.

Kanninen, M. F., O'Donoghue, P. E., Green, S. T., Leung, C. P., Roy, S. and Burnside, O. H. (1991). Applications of advanced fracture mechanics to fuselage structures. In *Structural Integrity of Aging Airplanes* (Edited by S. N. Atluri, S. G. Sampath and P. Tong), pp. 213–224. Springer, Berlin.

Kanninen, M. F., Leung, C. P., O'Donoghue, P. E., Morrow, T. B., Popelar, C. F., Buzzichelli, G., Demofonti, G., Hadley, I., Rizzi, L. and Venzi, S. (1992). The development of a ductile pipe fracture model. Report submitted to the Pipeline Research Committee, American Gas Association, Arlington, Virginia.

Kanninen, M. F., Grant, T. S., Demofonti, G. and Venzi, S. (1993a). The development and validation of a theoretical ductile fracture model. *Proceedings of the Eighth Symposium on Line Pipe Research, Houston, Texas*. American Gas Association, Arlington, Virginia.

Kanninen, M. F., Kuhlman, C. J. and Mamoun, M. M. (1993b). Rupture-prevention design procedure to ensure PE gas pipe system performance. *Proceedings of the Thirteenth International Plastic Fuel Gas Pipe Symposium, San Antonio, Texas*, pp. 182–193. American Gas Association, Arlington, Virginia.

Kiefner, J. F., Maxey, W. A., Eiber, R. J. and Duffy, A. R. (1973). Failure stress levels of flaws in pressurized cylinders. In *Progress in Flaw Growth and Fracture Toughness Testing*. American Society for Testing and Materials, ASTM STP536, pp. 461–481.

Knauss, W. G. and Rosakis, A. J. (Editors) (1990). *Non-Linear Fracture*. Kluwer Academic, Dordrecht.

Moran, B. and Shih, C. F. (1987). Crack tip and associated domain integrals from momentum and energy balance. *Engng Fracture Mech.* **27**, 615–642.

O'Donoghue, P. E., Green, S. T., Kanninen, M. F. and Bowles, P. K. (1991). Development of a fluid–structure interaction model for flawed fluid containment boundaries with applications to gas transmission and distribution piping. *Comput. Struct.* **38**, 501–513.

Priest, A. H. and Holmes, B. (1981). A multi-test piece approach to fracture characterization of linepipe steels. *Int. J. Fracture* **17**, 277–299.

Ramulu, M. and Kobayashi, A. S. (1983). Dynamic crack curving—a photoelastic evaluation. *Exp. Mech.* **23**, 1–9.

Report of the President's Commission on Aviation Security and Terrorism (1990). Washington, D.C.

Shimamoto, A., Kosai, M. and Kobayashi, A. S. (1994). Crack arrest at a tear strap under mixed mode loading. *Engng Fracture Mech.* **47**, 59–74.

Sih, G. C. (1974). Strain-energy-density factor applied to mixed-mode crack problems. *Int. J. Fracture Mech.* **10**, 305–321.

Streit, R. and Finnie, I. (1980). An experimental investigation of crack path directional stability. *Exp. Mech.* **20**, 17–23.

Swift, T. (1987). Damage tolerance in pressurized fuselages. *14th Symposium International Comm. Aeronautical Fatigue*. Ottawa, Canada, 10–12 June.

Swift, T. (1992). Unarrested fast fracture. In *Durability of Metal Aircraft Structures* (Edited by S.N. Atluri *et al.*). Atlanta Technology Publications.

Taylor, G. I. (1963). The fragmentation of tubular bombs. In *Scientific Papers of G.I. Taylor*, Vol. III, pp. 387–390. Cambridge Press, Cambridge.

U.K. Air Accidents Investigation Branch (1990). Report on the accident to Boeing 747-121-W739PA at Lockerbie, Dumfriesshire, Scotland on 21 December 1988. Aircraft Accident Report 2/90, HMSO, London.

Venzi, S., Martinelli, A. and Re, G. (1981). Measurement of fracture initiation and propagation parameters from fracture kinematics. In *Analytical and Experimental Fracture Mechanics* (Edited by G.C. Sih and M. Mirabile), pp. 737–756. Sijthoff and Noordhoff.

Yayla, P. and Leevers, P. S. (1989). A new small scale pipe test for rapid crack propagation. *Proceedings of the Eleventh Plastic Fuel Gas Pipe Symposium*, pp. 344–353. American Gas Association, Arlington, Virginia.